Detection of P-Glycoprotein Activity in Endotoxemic Rats by ^{99m}Tc-Sestamibi Imaging

Jing-Hung Wang, MSc[1]; Deborah A. Scollard, BSc[2]; Shirley Teng, MSc[1]; Raymond M. Reilly, PhD[1,2]; and Micheline Piquette-Miller, PhD[1]

[1]Department of Pharmaceutical Sciences, University of Toronto, Toronto, Ontario, Canada; and [2]Division of Nuclear Medicine, University Health Network, Toronto, Ontario, Canada

^{99m}Tc-sestamibi is a widely used radiopharmaceutical agent for myocardial and oncologic imaging. Because of its unique role as a P-glycoprotein (Pgp)–specific substrate, this compound can be used to examine Pgp functional activity in vitro and in vivo under pathologic conditions. Our objective was to use ^{99m}Tc-sestamibi as a tool to investigate whether systemic inflammation induced by *Escherichia coli* lipopolysaccharide (LPS) would affect in vivo Pgp function in the brain, heart, liver, and kidneys of rats. Moreover, we also wanted to examine LPS-mediated effects in the placenta of pregnant rats because of the limited amount of in vivo data on this tissue. **Methods:** Rats were injected intraperitoneally with LPS or an equal volume of saline as controls. After certain time periods (6 or 24 h), animals were administered 20 MBq of ^{99m}Tc-sestamibi intravenously, and then images were taken at 0.5, 1, 2, and 3 h. Tissues of rats were excised for ^{99m}Tc-sestamibi biodistribution analysis by γ-counting and messenger RNA (mRNA) analysis by reverse transcription–polymerase chain reaction. Western blot analysis with antibody C-219 was used to detect Pgp levels. **Results:** LPS treatment for 6 h caused a significant downregulation of *mdr1a* mRNA levels in the brain, heart, and liver, whereas 24 h of LPS treatment significantly reduced *mdr1a* mRNA levels only in the liver. A significant downregulation of *mdr1a* mRNA was seen in the brain, heart, and liver within 6 h after LPS administration. Imaging and biodistribution studies demonstrated a higher accumulation of ^{99m}Tc-sestamibi in the brain, heart, and liver of LPS-treated rats. In the brain, LPS-imposed downregulation of *mdr1a* mRNA levels was transient, with significant suppression at 4, 6, and 12 h, and the levels recovered to nearly normal by 24 h. This time-dependent downregulation of mRNA correlated with protein levels determined by Western blot analysis. Biodistribution studies of pregnant rats demonstrated a 3.5-fold-higher accumulation of ^{99m}Tc-sestamibi in the fetal tissues of LPS-treated pregnant rats than in saline-treated control rats. Furthermore, placental *mdr1a* and *mdr1b* mRNA levels were also significantly downregulated by LPS treatment. **Conclusion:** Our results indicate that LPS-induced systemic inflammation caused an increased retention of ^{99m}Tc-sestamibi in the brain, heart, liver, and fetal tissues. These results correlated with a reduction in *mdr1a* mRNA levels in each organ.

Key Words: radiopharmaceuticals; multidrug resistance; ATP-binding cassette transporters; inflammation

J Nucl Med 2005; 46:1537–1545

Inflammation is a systemic response to numerous stimuli, including infection, trauma, malignant growth, or ischemia, and can result in altered drug pharmacokinetics and pharmacodynamics (*1*). Experimentally, a rapid and reproducible inflammatory response is often elucidated by injection of the bacterial endotoxin lipopolysaccharide (LPS). Intraperitoneal injection of LPS is a well-characterized model of systemic inflammation. Systemic inflammation induced by turpentine or LPS administration has been shown to strongly suppress P-glycoprotein (Pgp) at the levels of protein, messenger RNA (mRNA), and functional activity in rat liver (*2*) and intestine (*3*). In the brain, Pgp has been shown to be downregulated by locally induced inflammation (*4*), but the impact of systemic inflammation has not been examined. Because of the extensive tissue expression of Pgp and its critical role in removing xenobiotics from cells and tissues, it is also important to understand the regulation of Pgp expression under systemic inflammatory conditions in various organs, such as the kidney, heart, placenta, and brain.

^{99m}Tc-sestamibi is a cationic radiopharmaceutical that is widely used for evaluating cardiac function and for tumor imaging. The accumulation of this compound is known to occur within cells in response to the physiologically negative mitochondrial and plasma membrane potentials (*5,6*). Sestamibi is also a well-known substrate for Pgp. In vitro studies have shown that the cellular efflux transport of sestamibi is correlated with the expression of Pgp and that the transport of sestamibi can be inhibited by several Pgp and multidrug resistance modulators, such as PSC-833 and VX-710 (*7,8*). Clinical in vivo studies also have established significant correlations between ^{99m}Tc-sestamibi efflux from tumors and Pgp expression in cancer patients (*9,10*). Moreover, the effectiveness of Pgp modulators also has been studied in vivo with ^{99m}Tc-sestamibi (*8,11,12*). Hence, the imaging of ^{99m}Tc-sestamibi distribution throughout the body may enable the in vivo tracing and mapping of specific transporter functions during chemo-

Received Mar. 29, 2005; revision accepted May 25, 2005.

For correspondence or reprints contact: Micheline Piquette-Miller, PhD, Department of Pharmaceutical Sciences, University of Toronto, 19 Russell St., Toronto, Ontario, Canada M5S 2S2.

E-mail: m.piquette.miller@utoronto.ca

therapy and may be a useful technique for monitoring the development of Pgp-mediated multidrug resistance.

Although ^{99m}Tc-sestamibi is widely used to detect in vivo Pgp activity in tumors, the application of ^{99m}Tc-sestamibi to the monitoring of endogenous Pgp activity in normal tissues has not been studied. A large variability in Pgp activity is seen clinically; therefore, the disposition of ^{99m}Tc-sestamibi likewise may be affected. ^{99m}Tc-sestamibi thus may be useful as an experimental model to study changes in Pgp activity in vivo in real time. Therefore, in this study, we investigated the effect of LPS treatment on rat Pgp expression and the correlation with ^{99m}Tc-sestamibi distribution in selected tissues. In particular, we were interested in evaluating the uptake of ^{99m}Tc-sestamibi in rat brain and fetal tissues to examine Pgp activity in the blood–brain barrier and placenta during systemic inflammation.

MATERIALS AND METHODS

Animals and Experimental Design

Male Sprague–Dawley rats (250–275 g) were purchased from Charles River Laboratories. All animal studies were conducted in accordance with the guidelines of the Canadian Council on Animal Care. Rats were injected intraperitoneally with endotoxin at 5 mg/kg (LPS from *Escherichia coli* serotype O55:B5; Sigma–Aldrich) or an equal volume of saline. Rats were used for ^{99m}Tc-sestamibi imaging studies as described below or sacrificed at selected time points (2, 4, 6, 12, and 24 h) after injection, and the brain, liver, heart, and kidneys were excised and frozen at −80°C for subsequent RNA isolation. Six animals were used for each group.

In a different set of experiments, pregnant female Sprague–Dawley rats were purchased from Charles River Laboratories. On day 17 of pregnancy, animals were administered LPS (0.5 or 1.0 mg/kg intraperitoneally) or an equal volume of saline and were injected with ^{99m}Tc-sestamibi 20 h later. At 24 h (4 h after ^{99m}Tc-sestamibi administration), the rats were sacrificed, and fetal tissues, placenta, and other organs were collected for ^{99m}Tc-sestamibi biodistribution studies.

Reverse Transcription (RT)–Polymerase Chain Reaction (PCR) Analysis of mRNA

RNA was extracted from tissues by use of a QuickPrep total RNA extraction kit (Amersham), and single-stranded complementary DNA (cDNA) was synthesized from 2.5 μg of RNA by use of a First Strand cDNA synthesis kit (MBI Fermentas) according to the manufacturer's protocol. Standard curves were generated to establish the optimal linear range of template concentrations for PCR, and 2.5 μg of RT product (cDNA template) were used for all PCRs. The cDNA templates were amplified in the presence of $MgCl_2$ at 1.5 mmol/L, deoxynucleoside triphosphates at 200 μmol/L, and 50 pmol of forward and reverse primers in a total volume of 50 μL by use of a GeneAmp 2400 Thermocycler (Perkin–Elmer). The reaction was initiated by the addition of 2.5 U of *Taq* polymerase (MBI Fermentas), and amplification proceeded through 25 cycles for the glyceraldehyde 3-phosphate dehydrogenase (GAPDH) gene and *mrp1* and through 30 cycles for *mdr1a* and *mdr1b*. The PCR products were separated by electrophoresis on 2% agarose gels, stained with SYBR Gold nucleic acid stain (Molecular Probes), and visualized under ultraviolet light. The sizes of DNA bands were confirmed by use of a Gene Ruler 100-base-pair DNA ladder (MBI Fermentas). Optical densities were normalized to GAPDH band intensities.

PCR primers were obtained from the DNA Synthesis Centre (Hospital for Sick Children), and their sequences were as follows: GAPDH forward, 5′-CCATCACCATCTTCCAGGAG-3′; GAPDH reverse, 5′-CCTGCTTCACCACCTTCTTG-3′; *mdr1a* forward, 5′-GATGGAATTGATAATGTGGACA-3′; *mdr1a* reverse, 5′-AAGGATCAGGAACAATAAA-3′; *mdr1b* forward, 5′-GA-AATAATGCTTATGAATCCCAAAG-3′; *mdr1b* reverse, 5′-GGTTTCATGGTCGTCGTCTCTTGA-3′; *mrp1* forward, 5′-TTCTAGTGTTGGACGAGGCT-3′; and *mrp1* reverse, 5′-TGGCCATGCTATAGAAGACG-3′. Significant findings from mRNA results were confirmed by real-time PCR.

Western Blot Analysis of Pgp Expression

Total membrane protein was isolated from 0.5 g of whole brain tissue in 5 mL of homogenate buffer (Tris [0.1 mol/L; pH 7.5] containing leupeptin [1 μg/mL], pepstatin [1 μg/mL], and phenylmethylsulfonyl fluoride [50 μg/mL]). After homogenization (Polytron homogenizer; Wheaton Science Products; 5 s, 10,000 rpm), homogenates were centrifuged at 1,500*g* for 20 min at 4°C. The supernatants were collected and centrifuged at 100,000*g* for 30 min at 4°C, and the pellets were suspended in 1 mL of homogenate buffer. Protein concentrations were measured spectrophotometrically with a protein assay (Bio-Rad Laboratories). Protein samples (20 μg) were separated in 6% sodium dodecyl sulfate–polyacrylamide gels and transferred to a Hybond nitrocellulose membrane (Amersham). The membrane was blocked overnight with Tris-buffered saline containing 0.05% Tween (TBS-T) and 5% nonfat milk at 4°C. After being washed with TBS-T, the membrane was incubated with either murine monoclonal antibody C-219 (1:500; Signet Laboratories) or mouse monoclonal anti–β-actin clone AC-15 (1:2,000; Sigma) for 2 h at room temperature. Blots were washed with TBS-T, incubated with antimouse horseradish peroxide antibody (1:2,000; Amersham) for 1 h, and washed with TBS-T. Bound antibody was detected by use of a Western blotting enhanced chemiluminescence detection kit (Amersham).

In Vivo Imaging of ^{99m}Tc-Sestamibi in LPS-Treated and Control Rats

The effect of inflammation on Pgp activity was evaluated in vivo by imaging with the Pgp substrate ^{99m}Tc-sestamibi. Rats were injected intraperitoneally with LPS or saline controls 6 h before imaging studies (LPS-6 group) or 24 h before imaging studies (LPS-24 group) as described earlier. Animals were anesthetized with a 0.4-mL mixture of ketamine:xylazine:acepromazine (100:5:10 mg/kg), and ^{99m}Tc-sestamibi (Bristol–Myers Squibb Medical Imaging) was administered (20 MBq in 0.2 mL) intravenously into a tail vein. Whole-body ventral images were acquired at 0.5, 1, 2, and 3 h after injection by use of a small–field-of-view γ-camera (TransCam; ADAC Laboratories Inc.) with a low-energy, general-purpose collimator. Static scintigraphy was performed for 300,000–500,000 counts (5–10 min) per frame in a 256 × 256 matrix with a 32-keV (22.8%) window set at approximately the 140-keV photopeak of ^{99m}Tc. Animals were sacrificed after the imaging at 3 h. Organs, including the blood, brain, heart, kidneys, and liver, were collected and weighed, and radioactivity was measured by use of a γ-counter (Cobra II series Auto-Gamma counting system model 5003; Packard Instrument Co.). Pregnant rats were sacrificed at 4 h after ^{99m}Tc-sestamibi administration. Fetuses and maternal organs, including the blood, brain, heart,

kidneys, liver, and placenta, were excised and weighed, and counts were determined as described above.

Data Analysis and Statistics

Regions of interest (ROIs) were drawn over the brain, heart, liver, soft tissue, and whole body for each animal at each imaging time point. Each ROI was expressed in counts per minute per pixel. The ROIs were normalized to the soft-tissue region for that same time point. The normalized values for the brain, heart, and liver were plotted at their respective times, that is, from 0.5 h to 3.0 h. The area under the curve (AUC) between these times (e.g., time 1 [t_1]) was calculated with the following formula:

$$AUC_{t_1-t_2} = [(I_1 + I_2) \times (t_2 - t_1)]/2,$$

where I_1 and I_2 represent the normalized counts per minute per pixel at t_1 and t_2, respectively. Total AUC values are the sum of the individual AUC values between 2 time points. The ROIs for the kidney were not analyzed because of errors from overlapping liver and intestine. The ROIs for the whole body served to monitor the excretion of the radiopharmaceutical from the rats.

Tissue radioactivity measured with the γ-counter was normalized as the percentage of the total dose injected into the animal. This calculation was based on both the recorded net injected dose of ^{99m}Tc-sestamibi for each animal and the radioactivity of the ^{99m}Tc-sestamibi internal standard measured at the same time in tissues. The results of tissue biodistribution analysis are reported as percentage injected dose per gram (%ID/g) of tissue. All imaging, biodistribution, and RT–PCR data are expressed as mean ± SEM. A 2-tailed *t* test was used for statistical comparison between groups. A difference in means with a *P* value of <0.05 was considered statistically significant.

RESULTS

Impact of Systemic Inflammation on *mdr1a* and *mdr1b* mRNA Expression

To search for LPS-induced changes in gene expression, the mRNA levels of the Pgp gene isoforms *mdr1a* and *mdr1b* were measured in samples isolated from the brain, heart, liver, and kidneys at 6 h after either saline or LPS administration (Fig. 1). Although *mdr1a* mRNA was detected in the brain, heart, liver, and kidneys, *mdr1b* mRNA was detected only in the liver and kidneys. LPS treatment

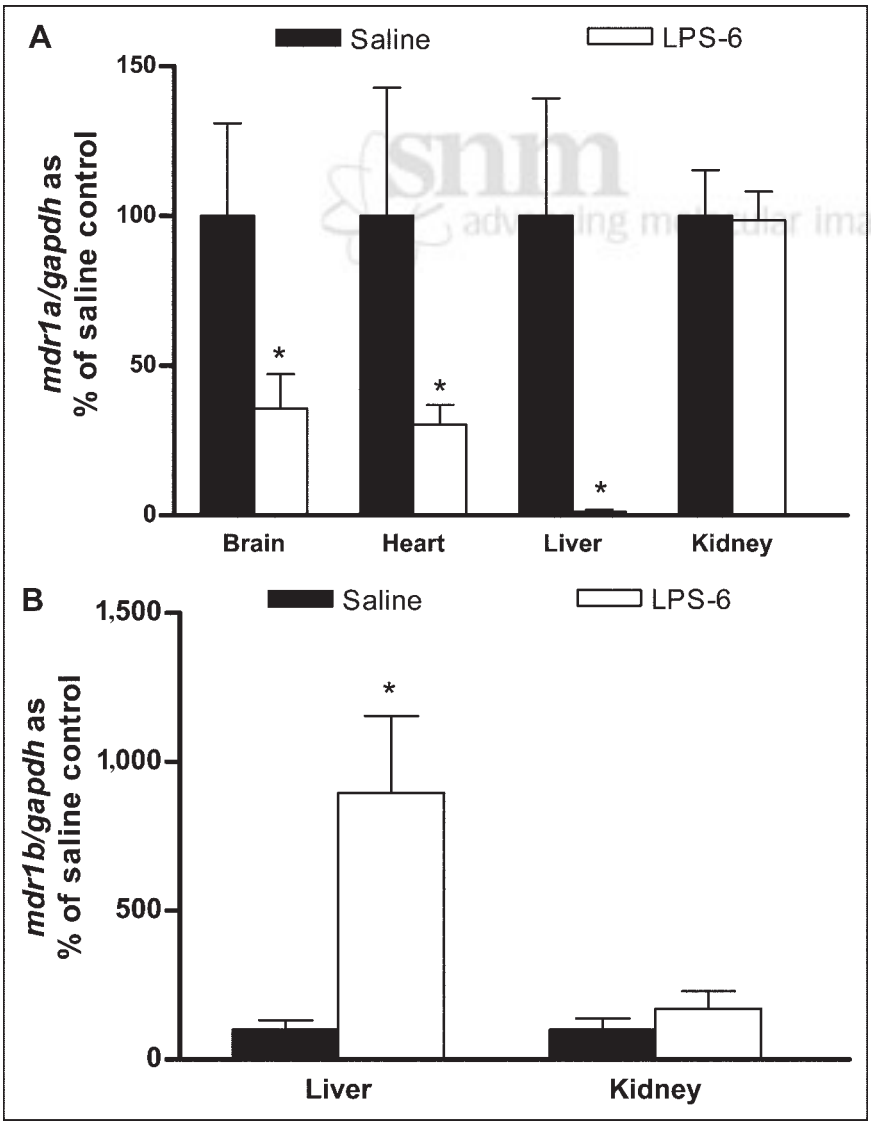

FIGURE 1. Effect of LPS-induced inflammation on *mdr1a* (A) and *mdr1b* (B) mRNA expression in brain, heart, liver, and kidneys in rats at 6 h after LPS treatment. Each PCR product was separated on 2% agarose gels, visualized under ultraviolet light, and normalized to GAPDH band of each sample. *mdr1b* mRNA levels in brain and heart were below detection limit. Bars represent mean ± SEM percent control value for 4–6 rats per group. Asterisk indicates *P* value of <0.05.

was found to impose significant reductions ($P < 0.05$) in *mdr1a* mRNA levels in the brain (64%), heart (67%), and liver (98%) but not in the kidneys (Fig. 1A). In contrast, a significant induction of *mdr1b* mRNA levels was seen in the liver and kidneys of both groups of LPS-treated rats (Fig. 1B). Downregulation appeared to be transient, as levels returned to nearly normal in most tissues at 24 h after LPS treatment (data not shown).

Effect of Systemic Inflammation on Biodistribution of ^{99m}Tc-Sestamibi

An increased retention of radioactivity was seen in most samples obtained from LPS-treated rats. Compared with those in the control group, the levels of ^{99m}Tc-sestamibi in the blood were significantly higher in the LPS-6 group but not in the LPS-24 group (Table 1). No significant correlations between levels in blood and accumulation in organs were seen in either LPS-treated or control animals (data not shown). Of note, the retention of ^{99m}Tc-sestamibi was higher in the brain of LPS-treated rats than in that of control rats, reaching significance in the LPS-24 group. The most significant changes in ^{99m}Tc-sestamibi accumulation were seen in the liver and kidneys of LPS-treated rats. Compared with that in control rats, radioactivity in the liver was significantly higher in both groups of LPS-treated rats. In the kidneys, there was a significantly higher accumulation of ^{99m}Tc-sestamibi in the LPS-6 group than in the control group. Radioactivity uptake was higher in the heart (between 2.5 and 3.7 %ID/g of tissue) than in other tissues examined; however, very little change in retention was observed after treatment with LPS compared with treatment with saline.

Effect of Systemic Inflammation on In Vivo Imaging with ^{99m}Tc-Sestamibi

Whole-body imaging was used to determine whether ^{99m}Tc-sestamibi can be used to noninvasively monitor Pgp activity in vivo. A representative scan is shown in Figure 2.

TABLE 1
^{99m}Tc-Sestamibi Biodistribution in Control and LPS-Treated Rats*

Time	Tissue	%ID/g of tissue		% Control value
		Saline	LPS	
6 h	Blood	0.013 ± 0.003	0.022 ± 0.002	167 ± 18†
	Brain	0.014 ± 0.004	0.019 ± 0.001	134 ± 6.1
	Heart	2.49 ± 0.39	3.02 ± 0.18	121 ± 7.2
	Liver	0.25 ± 0.05	0.85 ± 0.20	347 ± 81†
	Kidneys	0.93 ± 0.14	2.79 ± 0.46	300 ± 49†
24 h	Blood	0.024 ± 0.004	0.036 ± 0.003	150 ± 12
	Brain	0.022 ± 0.003	0.031 ± 0.001	141 ± 4.4†
	Heart	3.74 ± 0.24	3.49 ± 0.21	93 ± 5.5
	Liver	0.72 ± 0.07	1.92 ± 0.32	269 ± 45†
	Kidneys	1.98 ± 0.28	2.72 ± 0.36	137 ± 18

*Values represent mean ± SEM for 4–6 rats per group.
†$P < 0.05$.

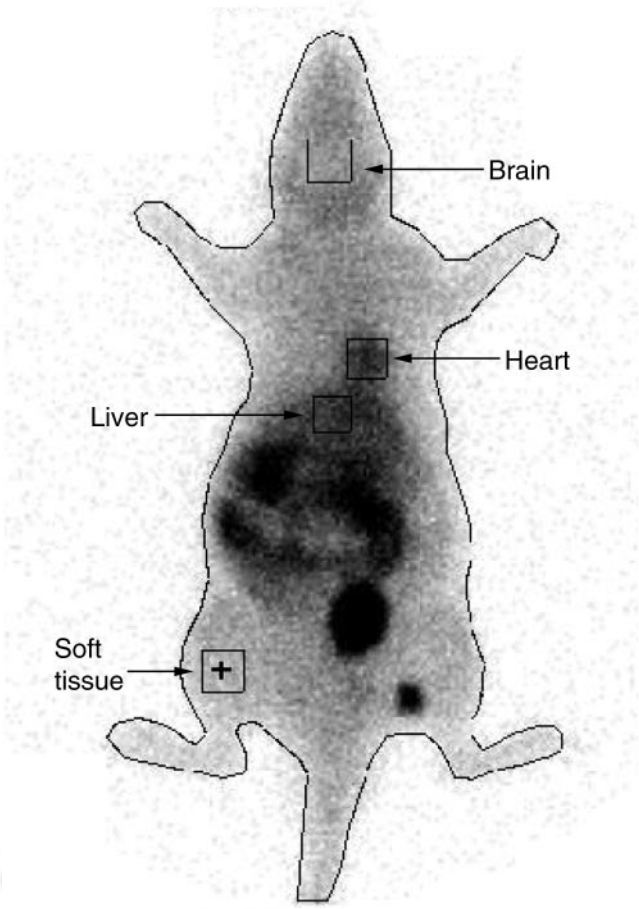

FIGURE 2. Representative scintigraphic image of control rat at 30 min after intravenous injection of ^{99m}Tc-sestamibi (20 MBq). ROIs are shown for each organ as well as whole body.

^{99m}Tc-sestamibi uptake in the brain, expressed as counts per minute per pixel, indicated that there was a moderate but insignificant increase in ^{99m}Tc-sestamibi uptake over the 3-h observation period in the LPS-6 group (Fig. 3A). On the other hand, in the LPS-24 group, there were significant differences in ^{99m}Tc-sestamibi uptake in the brain at all time points (Fig. 3B). Higher levels of ^{99m}Tc-sestamibi uptake also were seen in the heart area over 3 h in both the LPS-6 and the LPS-24 groups, with a significant effect seen at 1 h after ^{99m}Tc-sestamibi administration in the LPS-6 group (Figs. 3C and 3D). Compared with those in controls, higher levels of radioactivity were detected in the liver of LPS-treated rats (Figs. 3E and 3F).

Analysis of total AUC from 0.5 to 3 h demonstrated higher ^{99m}Tc-sestamibi levels in the brain, heart, and liver of LPS-treated rats than in those of control rats (Table 2). The total AUC in the brain was not significantly larger in the LPS-6 group but reached significance in the LPS-24 group. In the liver area, an increase in accumulation of more then 2.5-fold compared with that in the saline-treated group was observed in both the LPS-6 and the LPS-24 groups ($P < 0.05$). In the heart area, the AUC remained larger in the LPS-treated groups but did not reach significance.

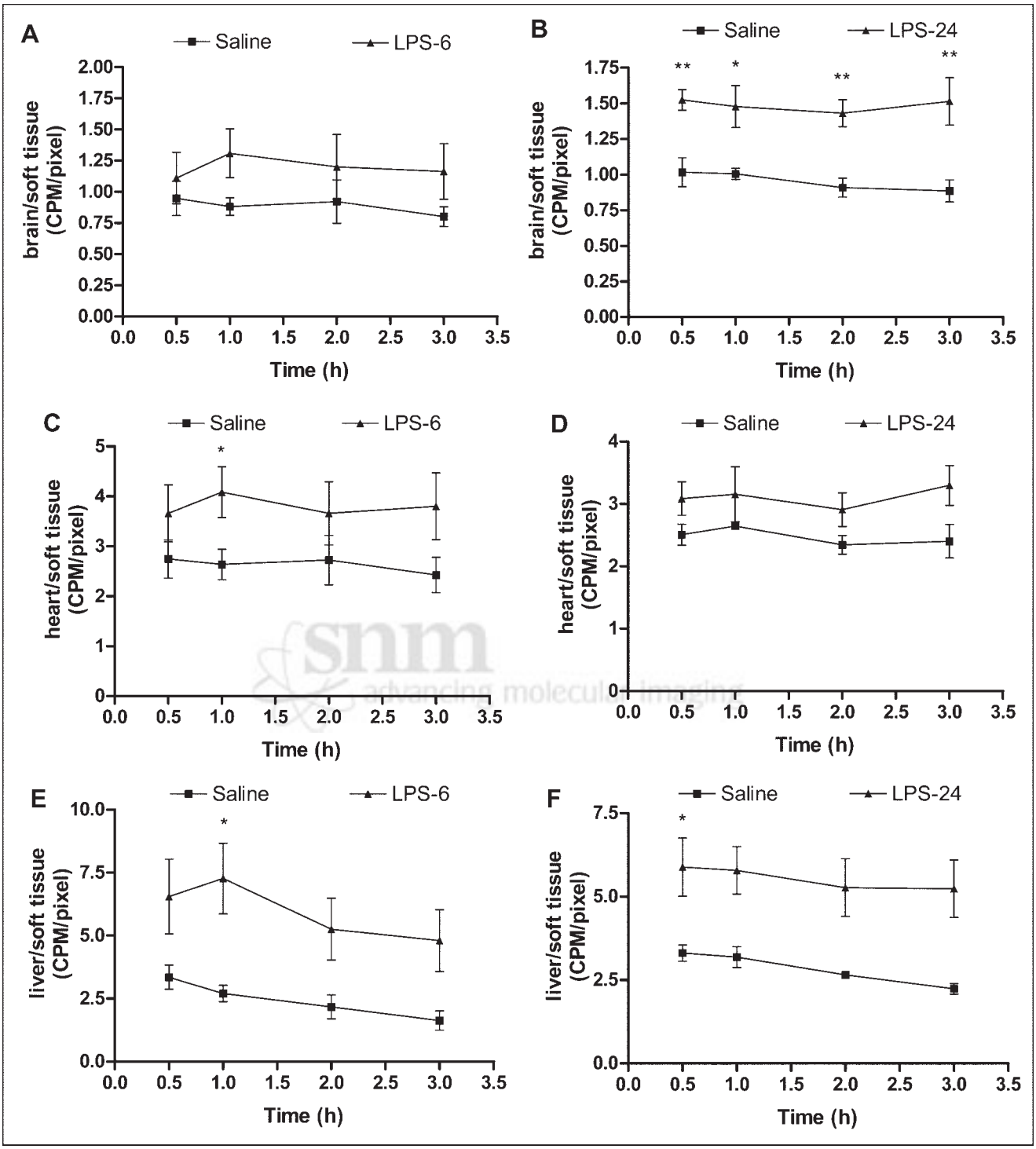

FIGURE 3. ^{99m}Tc-sestamibi imaging results in rats at 6 or 24 h after saline or LPS treatment. ROI analysis includes brain at 6 h (A) and 24 h (B), heart at 6 h (C) and 24 h (D), and liver at 6 h (E) and 24 h (F). Graphs represent radioactivity (counts per minute per pixel) in ROI of each organ at various time points normalized to that in corresponding soft-tissue region (counts per minute per pixel). Data points represent mean ± SEM for 4–6 rats per group. Asterisk indicates P value of <0.05; double asterisks indicate P value of <0.01.

Time Course of Inflammation-Induced Changes in Expression of Transporters in Brain

Levels of brain transporter mRNAs, including those of *mdr1a* and *mrp1*, were measured at different time points (2, 4, 6, 12, and 24 h) after the administration of LPS or saline. Figure 4A depicts *mdr1a* mRNA levels in the cerebrum. LPS treatment caused significant suppression of *mdr1a* mRNA levels at 4, 6, and 12 h, to 36%, 48%, and 54% the

TABLE 2
^{99m}Tc-Sestamibi Imaging AUC in Control and LPS-Treated Rats*

Time	Tissue	AUC from 0.5 to 3 h		
		Saline	LPS	% Control value
6 h	Brain	2.1 ± 0.3	3.1 ± 0.4	149 ± 21
	Heart	7.9 ± 1.1	11.4 ± 1.6	144 ± 20
	Liver	5.48 ± 0.86	15.8 ± 3.4	288 ± 62†
24 h	Brain	2.4 ± 0.1	3.7 ± 0.3	156 ± 12†
	Heart	6.2 ± 0.3	7.7 ± 0.8	125 ± 13
	Liver	6.5 ± 0.5	18.2 ± 4.5	279 ± 69†

*Values represent mean ± SEM for 4–6 rats per group.
†$P < 0.05$.

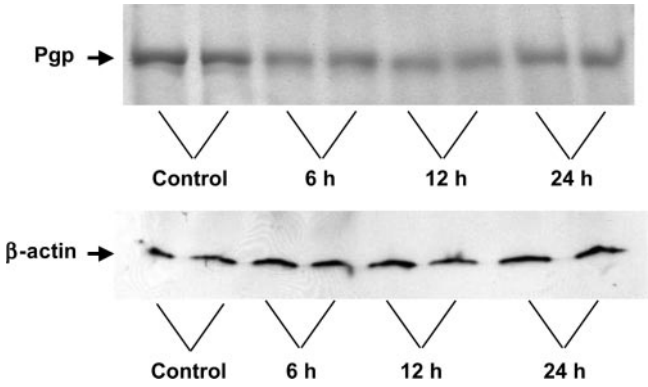

FIGURE 5. Representative Western blots of rat brain membrane protein with antibodies used to detect immunodetectable levels of Pgp (C-219) and β-actin at various times after LPS administration (6, 12, and 24 h). Control rats received saline.

levels in the saline-treated group, respectively. At 24 h, the *mdr1a* mRNA levels were restored almost to control levels. Levels of Pgp expression immunodetected with antibody C-219 also showed a transient downregulation of protein levels at 6 and 12 h, with a slight recovery by 24 h (Fig. 5).

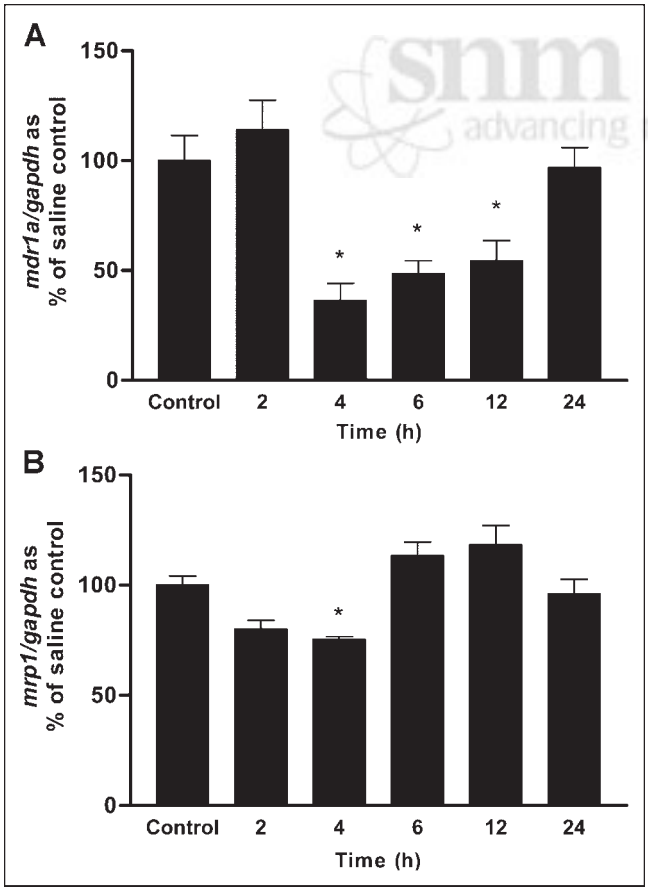

FIGURE 4. Time course of *mdr1a* (A) and *mrp1* (B) mRNA expression in cerebrum of LPS-treated rats. Control rats received saline. Bars represent mean ± SEM percent control value for 4–6 rats per group. Asterisk indicates *P* value of <0.05.

Because ^{99m}Tc-sestamibi is also a substrate for MRP1, we also examined the effect of LPS treatment on the expression of *mrp1* mRNA. Figure 4B displays *mrp1* mRNA levels in samples isolated from the cerebrum of saline- and LPS-treated rats. In LPS-treated animals, we found decreases in *mrp1* mRNA levels at 2 h ($P > 0.05$) and 4 h ($P < 0.05$); the levels returned to normal by 24 h.

Effect of Systemic Inflammation on ^{99m}Tc-Sestamibi Distribution in Pregnant Rats and Fetuses

Compared with the results obtained in control rats, the administration of LPS caused significant changes in *mdr1a* and *mdr1b* mRNA levels in the placenta of pregnant rats. Placental *mdr1a* mRNA levels were significantly downregulated to 43% the level in saline-treated rats ($P < 0.01$) by treatment with LPS at 0.5 mg/kg and to 13% the level in saline-treated rats ($P < 0.01$) by treatment with LPS at 1.0 mg/kg (Fig. 6A). *mdr1b* mRNA levels also were significantly downregulated to 28% the level in saline-treated rats ($P < 0.05$) by treatment with LPS at 0.5 mg/kg.

We examined ^{99m}Tc-sestamibi distribution to determine whether LPS-induced changes in *mdr1a* expression altered the placental transfer of ^{99m}Tc-sestamibi. The biodistribution results indicated that the average ratio of radioactivity in the fetus to that in the placenta was 3.5-fold higher ($P < 0.05$) (ratio in saline-treated rats, 2.23% ± 0.34%; ratio in LPS-treated rats, 7.74% ± 2.24%) in both LPS-treated groups than in the saline-treated group (Fig. 6B). There was no significant difference in ^{99m}Tc-sestamibi biodistribution between the 2 doses of LPS. Compared with saline treatment, 24 h of LPS treatment also resulted in higher radioactivity (%ID/g of tissue) being retained in maternal organs, including the blood (13.7-fold; $P < 0.05$), brain (1.5-fold; $P < 0.05$), liver (12.1-fold; $P < 0.01$), and kidneys (3.0-fold; $P > 0.05$).

DISCUSSION

In this study, the effect of systemic inflammation on Pgp functional activity was investigated in vivo with ^{99m}Tc-

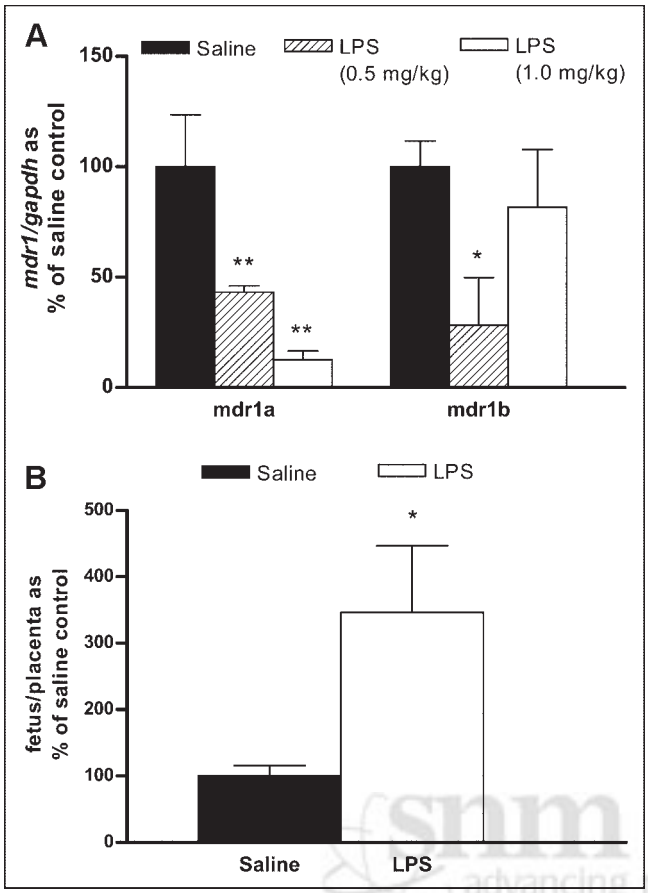

FIGURE 6. Effect of LPS-induced inflammation on expression of *mdr1* in placenta (A) and ratio of ^{99m}Tc-sestamibi radioactivity in fetus to that in placenta (B). LPS (0.5 or 1.0 mg/kg)-treated or saline (control)-treated pregnant rats were administrated 20 MBq of ^{99m}Tc-sestamibi intravenously and sacrificed 4 h later. Each pair of placenta and corresponding fetus was individually collected, separated, and processed for γ-counting or RNA isolation. Radioactivity content of each tissue was calculated as percent counts per minute per total dose per gram of tissue, and ratio of radioactivity in fetus to that in placenta was calculated. Bars represent mean ± SEM percent control value for 3–6 rats per group. Asterisk indicates *P* value of <0.05; double asterisks indicate *P* value of <0.01.

sestamibi as a specific substrate. Cellular uptake of ^{99m}Tc-sestamibi occurs through physiologic association with negatively charged mitochondrial, cytoplasmic, and plasma membrane potentials (*13*). Tissues with a larger number of mitochondria (e.g., heart, liver, kidneys, and tumor) retain a larger proportion of ^{99m}Tc-sestamibi and are more conspicuous in scintigraphic images (*14*). Although the cellular uptake of ^{99m}Tc-sestamibi is mainly attributable to membrane electron potentials and passive diffusion, transporters are known to play important roles in its cellular efflux and excretion. Recent studies have demonstrated that during inflammation, the expression of various transporters is altered in rodents. For example, previous reports described the downregulation of *mdr1a, mdr1b, mrp2,* and *spgp* mRNA expression as well as Pgp activity in liver (*2,15*), the suppression of *mdr1a* and *mrp2* mRNA expression and functional activity in intestine (*3*), and a decrease in the expression of *mdr1a* and *oatp2* in brain (*4*). Various studies have indicated that the release of proinflammatory cytokines, including tumor necrosis factor α, interleukin 1β, and interleukin 6, during the inflammatory response is primarily involved in mediating this downregulation (*15–18*). Because the Pgp/ABCB1 transporter has been shown to cause the efflux of ^{99m}Tc-sestamibi, this radiopharmaceutical may be a promising tool for the noninvasive in vivo imaging of Pgp function (*9,19*).

Overall, our results from these studies indicated that LPS-mediated inflammation in pregnant and nonpregnant rats was associated with a greater retention of ^{99m}Tc-sestamibi in the blood, brain, heart, and liver. Indeed, results from both ^{99m}Tc-sestamibi imaging and tissue biodistribution analyses indicated that LPS treatment induced an increase in the retention of ^{99m}Tc-sestamibi in several organs. These changes likely reflect decreased Pgp-mediated excretion and distribution of ^{99m}Tc-sestamibi. Because ^{99m}Tc-sestamibi is cleared from the body primarily through active Pgp-mediated secretion, increased levels in the blood of LPS-treated animals likely reflect decreased clearance attributable to inflammation-mediated downregulation of Pgp expression. Hence, increased accumulation in organs could be attributable in part to increased concentrations in the blood. However, changes in concentrations in the blood could not fully explain alterations in accumulation in organs. For example, biodistribution data for LPS-treated animals indicated a 40% increase in concentrations in blood but a 3.5-fold increase in accumulation in the liver. Furthermore, we did not detect significant correlations between levels in blood and accumulation in organs in either LPS-treated or control animals.

Consistent with the observed alterations in ^{99m}Tc-sestamibi distribution, decreased *mdr1a* expression was detected in many tissues of LPS-treated rats. Pgp is encoded by *mdr1a* and *mdr1b* in rodents. Indeed, the downregulation of *mdr1a* mRNA was seen in the brain, heart, and liver of LPS-treated rats, whereas *mdr1b* mRNA was upregulated in the liver. Although *mdr1a* was expressed at moderate to high levels in all tissues examined, *mdr1b* expression was undetectable in the brain and heart. Together, these results indicate that *mdr1a* may play a more dominant role than *mdr1b* in transporting ^{99m}Tc-sestamibi. ^{99m}Tc-sestamibi is also a low-affinity substrate for MRP1, and studies with cultured cells have reported MRP1-mediated transport (*11,20*). In our study, only slight changes in the expression of *mrp1* were detected, and these changes were not consistent with the observed changes in ^{99m}Tc-sestamibi distribution. Likewise, MRP1-mediated transport has not been detected clinically in vivo (*13*). Thus, changes in ^{99m}Tc-sestamibi disposition are likely to reflect primarily changes in Pgp activity.

Although changes in mRNA levels generally precede alterations in Pgp activity, previous studies with rats dem-

onstrated maximal suppression in the expression and activity of Pgp at 12 to 24 h after the administration of LPS (*2,3*). We detected increases in the retention of radiation within the blood, heart, liver, and kidneys of rats at 6 h after LPS administration. This finding suggests that LPS-mediated changes in the expression and activity of Pgp may occur more rapidly than previously thought. On the other hand, maximal changes in the accumulation of ^{99m}Tc-sestamibi in the brain were seen in rats at 24 h after LPS treatment. This finding may reflect slight differences in physiologic properties or time delays for regulation within the blood–brain barrier. Alternatively, differences in the extent of changes in ^{99m}Tc-sestamibi accumulation in these organs could reflect differences in the basal expression and activity of *mdr1a*/Pgp in these organs.

Although ^{99m}Tc-sestamibi is known to accumulate in certain organs, it is not known whether it can also freely bypass the blood–brain barrier and accumulate in brain tissue. On the other hand, ^{99m}Tc-sestamibi SPECT has been used clinically over the past decade to image malignant brain tumors (*21–24*) as well as to predict the expression of Pgp/*mdr1* in gliomas (*25*). The levels of radioactivity that we detected in brain tissue were relatively low compared with those in the liver, heart, and kidneys but were in the same range as the levels in the blood. The decreased expression of *mdr1a* mRNA seen in the brain of LPS-treated rats is consistent with imaging results that demonstrated a significantly higher retention of radioactivity in the brain region of the LPS-24 group. Likewise, Goralski et al. (*4*) also reported transient downregulation of *mdr1a* expression with decreased Pgp activity in rats given an intracranial injection of LPS. This finding further supports the utility of the ^{99m}Tc-sestamibi imaging technique for detecting in vivo Pgp activity in the brain.

To date, information on the transplacental transport of ^{99m}Tc-sestamibi from mother to fetus has not been reported. Our results indicated that the placenta prevented the majority of ^{99m}Tc-sestamibi from reaching the fetus, with the average ratio of radioactivity in the fetus to that in the placenta approximating 2% in control animals. During LPS-induced inflammation, the average ratio was significantly increased to 3.5-fold that in control animals. This result is also comparable to the placental *mdr1a* and *mdr1b* mRNA levels, in that the latter were significantly downregulated at 24 h after LPS treatment. These data suggest that placental Pgp plays an important role in preventing the fetal uptake of compounds such as ^{99m}Tc-sestamibi. Furthermore, LPS-induced inflammation may reduce the protective function of placental Pgp, in turn increasing the risks associated with drug use during pregnancy.

It is also important to consider the clinical impact of inflammatory conditions on ^{99m}Tc-sestamibi imaging results, particularly because this agent is commonly used for myocardial imaging. Previous reports indicated that Pgp and *mdr1* mRNA are expressed in the endothelium of heart arterioles and capillaries (*26*). Likewise, we detected *mdr1a* mRNA in the heart, albeit at a level much lower than those in the liver, kidneys, and brain (data not shown). Although the levels of *mdr1a* were significantly decreased in the heart in LPS-treated animals, this decrease imposed only slight changes in the biodistribution and imaging of ^{99m}Tc-sestamibi in cardiac tissue. The high affinity of ^{99m}Tc-sestamibi for cardiac tissue and the relatively low Pgp activity likely contributed to these findings. Therefore, inflammation-induced changes in Pgp activity are unlikely to have a pronounced clinical impact on myocardial imaging.

In summary, our study indicates that LPS-induced systemic inflammation causes alterations in the distribution and elimination of ^{99m}Tc-sestamibi. Changes in the distribution to the brain, heart, liver, and fetal tissues correlated with reductions in *mdr1a* mRNA expression. Hence, our data strongly support the notion that this phenomenon may be attributable to inflammation-mediated suppression of Pgp, which is known to be a major sestamibi efflux transporter. The expression and activity of Pgp have been shown to influence the accumulation of ^{99m}Tc-sestamibi in many organs. Hence, ^{99m}Tc-sestamibi imaging may be a useful and powerful tool for the noninvasive in vivo monitoring of Pgp activity in a variety of disease conditions.

CONCLUSION

In conclusion, our findings suggest that inflammatory conditions, such as trauma, injury, infection, or inflammatory disease, can alter the distribution and clearance of xenobiotics. Changes in the expression of transporters in the brain, liver, and intestine lead to functional changes in the distribution and accumulation of substrates, such as ^{99m}Tc-sestamibi. The fact that imaging results obtained with ^{99m}Tc-sestamibi correlated highly with changes in the expression of Pgp in several tissues further demonstrates the potential utility of ^{99m}Tc-sestamibi for noninvasively assessing Pgp function in vivo. Furthermore, the interpretation of ^{99m}Tc-sestamibi imaging results in patients with various inflammatory conditions should take these changes into consideration.

ACKNOWLEDGMENTS

Funding for this study was provided by a grant from the Canadian Institutes of Health Research (CIHR). Micheline Piquette-Miller is a recipient of the RX&D Health Research Foundation–CIHR Research Career Award.

REFERENCES

1. Slaviero KA, Clarke SJ, Rivory LP. Inflammatory response: an unrecognized source of variability in the pharmacokinetics and pharmacodynamics of cancer chemotherapy. *Lancet Oncol*. 2003;4:224–232.
2. Piquette-Miller M, Pak A, Kim H, Anari R, Shahzamani A. Decreased expression and activity of P-glycoprotein in rat liver during acute inflammation. *Pharm Res*. 1998;15:706–711.
3. Kalitsky-Szirtes J, Shayeganpour A, Brocks DR, Piquette-Miller M. Suppression of drug-metabolizing enzymes and efflux transporters in the intestine of endotoxin-treated rats. *Drug Metab Dispos*. 2003;30:845–852.
4. Goralski KB, Hartmann G, Piquette-Miller M, Renton KW. Downregulation of

mdr1a expression in the brain and liver during CNS inflammation alters the in vivo disposition of digoxin. *Br J Pharmacol*. 2003;139:35–48.
5. Piwnica-Worms D, Kronauge JF, Chiu ML. Uptake and retention of hexakis (2-methoxyisobutyl isonitrile) technetium(I) in cultured chick myocardial cells: mitochondrial and plasma membrane potential dependence. *Circulation*. 1990; 82:1826–1838.
6. Piwnica-Worms D, Rao V, Kronauge J, Croop J. Characterization of multidrug-resistance P-glycoprotein transport function with an organotechnetium cation. *Biochemistry*. 1995;34:12210–12220.
7. Chen CC, Meadows B, Regis J, et al. Detection of in vivo P-glycoprotein inhibition by PSC-833 using Tc-99m sestamibi. *Clin Cancer Res*. 1997;4:545–552.
8. Peck RA, Hewett J, Harding MW, et al. Phase I and pharmacokinetic study of the novel MDR1 and MRP1 inhibitor biricodar administered alone and in combination with doxorubicin. *J Clin Oncol*. 2001;19:3130–3141.
9. Sun SS, Hsieh JF, Tsai SC, Ho YJ, Lee JK, Kao CH. Expression of mediated P-glycoprotein multidrug resistance related to Tc-99m MIBI scintimammography results. *Cancer Lett*. 2000;153:95–100.
10. Filipits M, Suchomel RW, Dekan G, et al. MRP and MDR1 gene expression in primary breast carcinomas. *Clin Cancer Res*. 1996;2:1231–1237.
11. Hendrikse NH, Franssen EJ, van der Graal WT, et al. Tc-99m-Sestamibi is a substrate for P-glycoprotein and the multidrug resistance-associated protein. *Br J Cancer*. 1998;77:353–358.
12. Zhou J, Higashi K, Ueda Y, et al. Expression of multidrug resistance protein and messenger RNA correlate with ^{99m}Tc-MIBI imaging in patients with lung cancer. *J Nucl Med*. 2001;42:1476–1483.
13. Sharma V, Luker G, Piwnica-Worms D. Molecular imaging of gene expression and protein function in vivo with PET and SPECT. *J Magn Reson Imaging*. 2002;16:336–351.
14. Maffioli L, Gasparini M, Chiti A, et al. Clinical role of technetium-99m sestamibi single-photon emission tomography in evaluating pretreated patients with brain tumours. *Eur J Nucl Med*. 1996;23:308–311.
15. Hartmann G, Kim H, Piquette-Miller M. Regulation of the hepatic multidrug resistance gene expression by endotoxin and inflammatory cytokines in mice. *Int Immunopharmacol*. 2001;1:189–199.
16. Hartmann G, Cheung A, Piquette-Miller M. Inflammatory cytokines, but not bile acids, regulate expression of murine hepatic anion transporters in endotoxemia. *J Pharmacol Exp Ther*. 2002;303:273–281.
17. Warren G, Van Ess P, Watson A, Mattson M, Blouin R. Cytochrome P450 and antioxidant activity in interleukin-6 knockout mice after induction of the acute-phase response. *J Interferon Cytokine Res*. 2001;21:821–826.
18. Lee G, Piquette-Miller M. Influence of IL-6 on MDR and MRP-mediated multidrug resistance in human hepatoma cells. *Can J Physiol Pharmacol*. 2001; 79:876–884.
19. Kao CH, Tsai SC, Liu TJ, et al. P-Glycoprotein and multidrug resistance-related protein expressions in relation to technetium-99m methoxyisobutylisonitrile scintimammography findings. *Cancer Res*. 2001;61:1412–1414.
20. Chen WS, Luker KE, Dahlheimer JL, Pica CM, Luker GD, Piwnica-Worms D. Effects of MDR1 and MDR3 P-glycoproteins, MRP1, and BCRP/MXR/ABCP on the transport of ^{99m}Tc-tetrofosmin. *Biochem Pharmacol*. 2000;60:413–426.
21. O'Tuama LA, Treves ST, Larar JN, et al. Thallium-201 versus technetium-99m-MIBI SPECT in evaluation of childhood brain tumors: a within-subject comparison. *J Nucl Med*. 1993;34:1045–1051.
22. Tomura N, Hirano H, Watanabe O, et al. Preliminary results with technetium-99m MIBI SPECT imaging in patients with brain tumors: correlation with histological and neuroradiological diagnoses and therapeutic response. *Comput Med Imaging Graph*. 1997;21:293–298.
23. Soler C, Beauchesne P, Maatougui K, et al. Technetium-99m sestamibi brain single-photon emission tomography for detection of recurrent gliomas after radiation therapy. *Eur J Nucl Med*. 1998;25:1649–1657.
24. Ak I, Gulbas Z, Altinel F, Vardareli E. Tc-99m MIBI uptake and its relation to the proliferative potential of brain tumors. *Clin Nucl Med*. 2003;28:29–33.
25. Yokogami K, Kawano H, Moriyama T, et al. Application of SPET using technetium-99m sestamibi in brain tumours and comparison with expression of the MDR-1 gene: is it possible to predict the response to chemotherapy in patients with gliomas by means of ^{99m}Tc-sestamibi SPET? *Eur J Nucl Med*. 1998;25:401–409.
26. Meissner K, Sperker B, Karsten C, et al. Expression and localization of P-glycoprotein in human heart: effects of cardiomyopathy. *J Histochem Cytochem*. 2002;50:1351–1356.